

# Disposition Requirements for Binding in Aqueous Solution of Polar Substrates in the Cyclohexaamylose Cavity

Raymond J. Bergeron,\* Michael Almy Channing, George J. Gibeily, and David M. Pillor

Contribution from the Department of Chemistry, University of Maryland, College Park, Maryland 20742. Received December 20, 1976

**Abstract:** The extent to which cyclohexaamylose binds *p*-nitrophenol, 2,6-dimethyl-4-nitrophenol, 3,5-dimethyl-4-nitrophenol, 3-methyl-4-nitrophenol, and their corresponding sodium phenolates is shown to be dependent on how effectively the substrate can penetrate the cavity nitro group first. These results both bear out earlier intermolecular nuclear Overhauser effect studies on cycloamylose-substrate penetration and establish asymmetric penetration as a general phenomenon experienced by substituted *p*-nitrophenol and sodium *p*-nitrophenolate guests. Furthermore, these findings strongly suggest that the release of cycloamylose strain energy and/or expulsion of high-energy cavity water is not the major component in the overall forces responsible for substrate complexation of polar substrates. The differences in the dissociation constants for the cyclohexaamylose-substrate complexes investigated point to the importance of dipole-induced dipole interactions in the binding energy.

Although the cycloamyloses have received a great deal of attention as enzyme active-site models,<sup>1,2</sup> until now little of this interest has been focused on the nature of, and the forces responsible for, substrate complexation. Most of the emphasis has been on improving the cycloamyloses' catalytic ability<sup>3,4</sup> and expanding their spectrum of catalysis.<sup>5</sup> However, by studying the cycloamylose-substrate disposition in solution, we have been able to determine a great deal about the cycloamylose-substrate binding energy.

In an earlier experiment by measurement of both the changes in the <sup>1</sup>H and <sup>13</sup>C NMR spectra of the substrate and cycloamylose molecules in the complex and of an intermolecular nuclear Overhauser effect, we were able to show that both the *p*-nitrophenol and sodium *p*-nitrophenolate guests only partially penetrate the cyclohexaamylose cavity.<sup>6,7</sup> We found the penetration to be nitro end first, although just exactly how necessary this orientation is to binding was unclear.

Having demonstrated the direction and the extent to which these substrates penetrate the cyclohexaamylose cavity in solution, it became possible to design experiments which would indeed allow us to evaluate some of the forces suggested to be responsible for cycloamylose-substrate binding.

In this paper we report on our efforts to determine if asymmetric penetration of the cyclohexaamylose cavity by *p*-nitrophenol and sodium *p*-nitrophenolate-like substrates is a general phenomenon and a requisite for substrate binding, and we evaluate the binding theories in light of our results. We show that of the three current theories put forth to explain the origins of the cycloamylose-substrate binding energy, relief of cycloamylose strain energy,<sup>8</sup> release of high-energy cycloamylose cavity water,<sup>9</sup> and London dispersion forces,<sup>9</sup> the strain energy and the high-energy water concept are not in keeping with our observations.

## Experimental Section

**Materials.** The cyclohexaamylose, *p*-nitrophenol, 3-methyl-4-nitrophenol, and 2,6-dimethyl-4-nitrophenol were obtained from Aldrich Chemical Company. The *p*-nitrophenol was crystallized from chloroform while the 3-methyl-4-nitrophenol and the 2,6-dimethyl-4-nitrophenol were purified by high vacuum sublimation. The 3,5-dimethyl-4-nitrophenol was synthesized by the nitration of 3,5-dimethylphenol with nitric acid.<sup>10</sup> The resulting 3,5-dimethyl-4-nitrophenol was crystallized several times from chloroform/hexane (mp 107–108 °C; lit. mp 107–108 °C).<sup>10</sup>

**Sample Preparation.** Stock solutions of cyclohexaamylose were made up in trisodium phosphate buffer (pH 11.0 ± 0.02, *I* = 0.5) and in disodium phosphate buffer (pH 6.5 ± 0.02, *I* = 0.5). The pH was

adjusted with phosphoric acid. The substituted *p*-nitrophenol and substituted sodium *p*-nitrophenolate samples were made up in the same pH 6.5 ± 0.02 and 11.0 ± 0.02 buffer solutions, respectively.

**Sample Preparation for Nuclear Magnetic Resonance.** The cyclohexaamylose hydroxyl protons were exchanged for deuterium by lyophilizing 600 mg of the carbohydrate from 40 mL of D<sub>2</sub>O three times. This helps to minimize the HOD in the final sample. The buffer solutions were made up with anhydrous Na<sub>3</sub>PO<sub>4</sub> and Na<sub>2</sub>HPO<sub>4</sub> in D<sub>2</sub>O and the pD was adjusted with deuteriophosphoric acid. The final pD values were 11.0 ± 0.02 and 6.5 ± 0.02 with *I* = 0.5 in both buffers. These pD values were obtained by adding 0.4 to the pH meter reading,<sup>11</sup> using a combination electrode which had been standardized with pH 10.0 ± 0.003 buffer in H<sub>2</sub>O and then rinsed with D<sub>2</sub>O.

**Determination of Cycloamylose-Substrate Binding Constants by the Visible Spectra Method.** The change in absorbance of the various substituted *p*-nitrophenols and sodium *p*-nitrophenolates was measured as a function of cycloamylose concentration using a Cary Model 14 recording spectrophotometer with the cell compartment thermostated at 25 °C.

The data were treated according to the Hildebrand-Benesi<sup>12</sup> procedure plotting  $C_0S_0/\Delta\text{ABS}$  vs.  $C_0 + S_0$  providing a slope of  $1/\Delta\epsilon$  and an intercept of  $K_{\text{diss}}/\Delta\epsilon$ . In order to meet the requirement for a linear Hildebrand-Benesi plot (Appendix A), i.e.,  $[C_0][S_0] \ll [C_0S_0]^2$ , the concentration of the substrates was held at least ten times lower than the lowest cyclohexaamylose concentration. All of the data in this paper were analyzed with a least-squares linear regression program and only  $K_d$  values with high residual ratios were accepted.

**Determination of Cycloamylose-Substrate Dissociation Constants by Optical Rotation Method.** The change in optical rotation of cyclohexaamylose was measured as a function of changing substrate concentration using a Perkin-Elmer Model 241 polarimeter with a 10-cm cell thermostated at 25 °C. The cyclohexaamylose concentration was held constant at  $1.6 \times 10^{-4}$  M and the substrate concentrations were varied between 0.008 and 0.050 M. The data were also handled according to the Hildebrand-Benesi treatment;  $C_0S_0/\Delta\text{ROT}$  was plotted against  $C_0 + S_0$ . The  $K_d$  was obtained by dividing the intercept by the slope.<sup>13</sup>

**Determination of Cycloamylose-Substrate Dissociation Constants by Nuclear Magnetic Resonance.** <sup>1</sup>H-pulsed Fourier transform NMR spectra (100.1 MHz) were obtained on a Varian XL-100 spectrometer at 23 ± 0.5 °C. The change in chemical shift of the substrate aromatic protons was measured as a function of changing cycloamylose concentration. The sodium 3-methyl-4-nitrophenolate, sodium 3,5-dimethyl-4-nitrophenolate, and sodium 2,6-dimethyl-4-nitrophenolate substrates were made up in phosphate buffer at pD 11.0 ± 0.02, *I* = 0.5. The concentrations of the phenolates were held constant at 0.005, 0.006, and 0.005 M, respectively, and the cyclohexaamylose concentrations were varied between 0.005–0.050, 0.002–0.075, and 0.005–0.050 M, respectively. The data were treated according to a modified Hildebrand-Benesi equation (Appendix A). Because of the

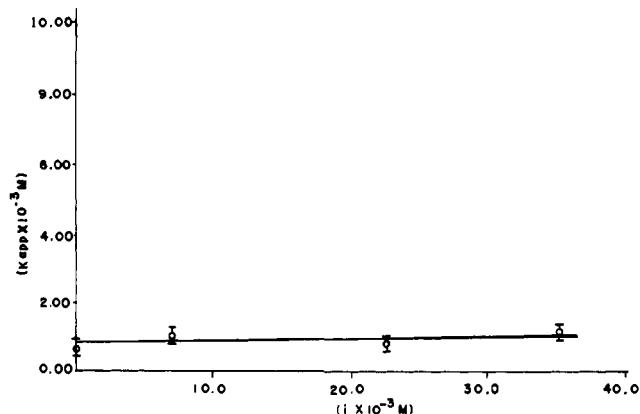


**Figure 1.** A plot of the apparent cyclohexaamylose-sodium *p*-nitrophenolate dissociation constants at different sodium 3,5-dimethyl-4-nitrophenolate inhibitor concentrations.

low solubility of the phenols, the dissociation constants for cycloamylose-phenol complexes were not measured with this technique.

**Inhibition of Sodium *p*-Nitrophenolate-Cyclohexaamylose Binding by Sodium 3,5-Dimethyl-4-nitrophenolate.** The binding of sodium *p*-nitrophenolate to cyclohexaamylose in phosphate buffer at pH 11.00,  $I = 0.5$ , was measured as described above at three separate concentrations of sodium 3,5-dimethyl-4-nitrophenolate, 0.007, 0.023, and 0.035 M, respectively. The apparent binding constants determined by Hildebrand-Benesi treatment of the data were plotted against the inhibitor concentrations (sodium 3,5-dimethyl-4-nitrophenolate) (Figure 1).

**Sodium 2,6-Dimethyl-4-nitrophenolate and Sodium 3,5-Dimethyl-4-nitrophenolate-Induced Shifts in the  $^1\text{H}$  NMR of Cyclohexaamylose.** The changes in the  $^1\text{H}$  NMR of cyclohexaamylose as induced by substrate complexation were measured on a 220-MHz NMR with the substrate concentrations held at 0.002 M and the cyclohexaamylose concentrations held at 0.045 M. The samples were run at  $25 \pm 1$  °C in phosphate buffer ( $\text{D}_2\text{O}$ ) at  $\text{pD } 11.0 \pm 0.02$ ,  $I = 0.5$ , with a sodium acetate external reference.

**Computer Simulation of Binding Curves.** A series of computer-simulated curves was generated for a simple  $\text{A} + \text{B} \rightleftharpoons \text{AB}$  binding model plotting  $[\text{AB}]$  vs.  $[\text{A}]/[\text{B}]$  for a number of different dissociation constants. The concentrations of A and B used in the simulation were in the same range as the experimental values. The experimental  $^1\text{H}$  NMR data corresponding to the sodium 2,6-dimethyl-4-nitrophenolate-cyclohexaamylose complex were plotted relative to computer values generated for an AB complex with a similar  $K_D$ . This was done by multiplying each of the experimental  $^1\text{H}$  NMR chemical-shift values by a constant obtained by dividing the observed chemical shift at a point where  $\Delta\delta_{\text{obsd}}/\Delta(\text{CD}/S) = 0$  by a number from the simulated curve at a point where  $\Delta\delta/\Delta(\text{CD}/S) = 0$ . This constant was also used to convert the sodium 3,5-dimethyl-4-nitrophenolate  $^1\text{H}$  NMR data.

## Results

**Cyclohexaamylose Binding of 2,6-Dimethyl-4-nitrophenol and Sodium 2,6-Dimethyl-4-nitrophenolate.** The changes in the visible spectra of both 2,6-dimethyl-4-nitrophenol and sodium 2,6-dimethyl-4-nitrophenolate, measured as a function of an increasing cycloamylose/substrate ratio, indicated strong substrate binding. The 2,6-dimethyl-4-nitrophenol-cyclohexaamylose complex has isosbestic points at 4732 and 3731 Å while the sodium 2,6-dimethyl-4-nitrophenolate-cyclohexaamylose complex has isosbestic points at 4220 and 4451 Å, respectively, indicating a one-to-one complex. A plot of the data in the form of  $[\text{C}_0][\text{S}_0]/\Delta\text{ABS}$  vs.  $[\text{C}_0] + [\text{S}_0]$  showed excellent straight line fits indicating an  $\text{A} + \text{B} \rightleftharpoons \text{AB}$  equilibrium model was likely (Appendix A). The sodium 2,6-dimethyl-4-nitrophenolate-cyclohexaamylose complex in pH  $11.0 \pm 0.02$  phosphate buffer ( $I = 0.5$ ) at 25 °C has a  $K_D$  of  $9.42 \pm 1.1 \times 10^{-4}$  M while the 2,6-dimethyl-4-nitrophenol-cyclohexaamylose complex at pH  $6.5 \pm 0.02$  ( $I = 0.5$ ) at 25

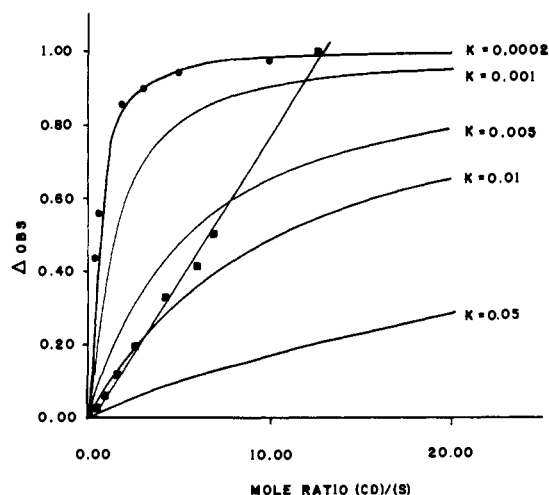


**Figure 2.** Computer-simulated binding curves for a simple  $\text{A} + \text{B} \rightleftharpoons \text{AB}$  equilibrium with different dissociation constants. The ratio of  $(\text{CD})/S$  is plotted against  $[\text{CS}]$  or the related changing observable. The  $^1\text{H}$  NMR data for the sodium 2,6-dimethyl-4-nitrophenolate- (●) and sodium 3,5-dimethyl-4-nitrophenolate- (■) cyclohexaamylose complexes are normalized and plotted.

**Table I.** Changes in Chemical Shifts of the Sodium *p*-Nitrophenolate 2 and 3 Protons and the Sodium 2,6-Dimethyl-4-nitrophenolate's Meta and Methyl Protons on Cyclohexaamylose Complexation

Substrate	% bound	2-H shift	3-H shift	2,6- $\text{CH}_3$ shift
	80.0	8.0	23.2	
	85.5	11.0	30.0	
	99	14.0	35.1	
	82.1		33.89	15.52
	96.4		38.06	17.62
	99.0		40.78	18.80

°C has a  $K_D$  of  $1.76 \pm 0.18 \times 10^{-3}$  M.

The dissociation constant for the sodium 2,6-dimethyl-4-nitrophenolate-cyclohexaamylose complex was also measured using both optical rotation ( $K_D = 1.42 \pm 0.58 \times 10^{-3}$  M at 25 °C) and  $^1\text{H}$  NMR as probes ( $K_D = 1.96 \pm 0.53 \times 10^{-4}$  M at 23 ± 0.5 °C). Optical rotation changes generated in the cavity were measured as a function of increasing substrate/cycloamylose ratios, while changes in the substrate's  $^1\text{H}$  NMR were measured as a function of increasing cycloamylose/substrate ratios. Both sets of data when plotted according to modified Hildebrand-Benesi equations gave straight lines with correlation coefficients > 0.9970 further supporting a simple  $\text{A} + \text{B} \rightleftharpoons \text{AB}$  equilibrium.

It is noteworthy that the aromatic protons of sodium 2,6-dimethyl-4-nitrophenolate undergo nearly twice the contact shifts as the methyl protons (Table I) just as we observed earlier that the meta protons of sodium *p*-nitrophenolate sustained nearly twice the contact shift as the ortho protons.<sup>6</sup>

Since no internal line-width standard was used, the line broadening of the sodium 2,6-dimethyl-4-nitrophenolate resonances could not be accurately assessed. No internal line-width standard was available, since the possibility existed that any small molecule added to the solutions to provide such a standard would compete with the cavity for a binding site.

### Effect of Sodium 2,6-Dimethyl-4-nitrophenolate and Sodium

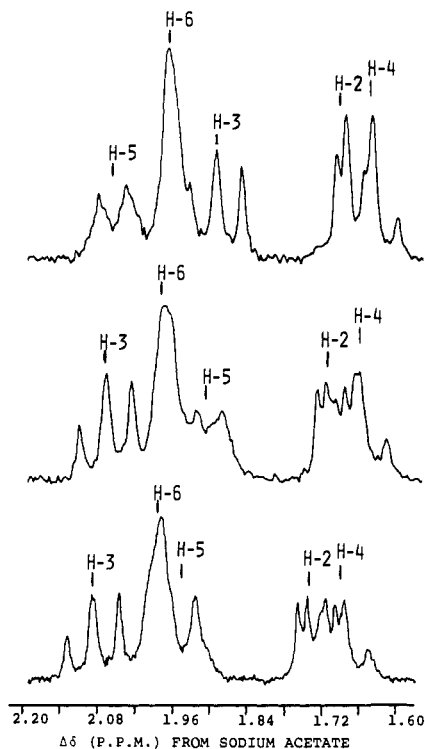


**Figure 3.**  $^1\text{H}$  NMR (220 MHz) of: (bottom) cyclohexaamylose; (middle) sodium 3,5-dimethyl-4-nitrophenolate-cyclohexaamylose complex; (top) sodium 2,6-dimethyl-4-nitrophenolate-cyclohexaamylose complex. The anomeric protons are not shown.

**3,5-Dimethyl-4-nitrophenolate on the Cyclohexaamylose Nuclear Magnetic Resonance Spectra.** The spectrum of free cycloheptamylose as well as the spectrum for a variety of cycloheptamylose aromatic complexes were assigned by Demarco and Thakker.<sup>14</sup> They demonstrated that upon complexation of any of several aromatic guests, the cycloheptamylose H-3 and especially the H-5 protons shifted upfield because of the diamagnetic anisotropy of the included benzenoid guests. We also observed this shift of the cycloheptamylose H-5 and H-3 protons on complexation of both *p*-nitrophenol and sodium *p*-nitrophenolate.<sup>6</sup> However, we demonstrated that only the H-3 protons were shielded in the cyclohexaamylose complexes, i.e., the substrate only partially penetrated the cavity.  $^1\text{H}$  NMR spectra (220 MHz) were obtained for both the sodium 2,6-dimethyl-4-nitrophenolate and the sodium 3,5-dimethyl-4-nitrophenolate-cyclohexaamylose complexes in  $\text{D}_2\text{O}$  (Figure 3). The spectra of the sodium 2,6-dimethyl-4-nitrophenolate-cyclohexaamylose complex with the cycloamylose 96% bound (assuming a dissociation constant of  $9.42 \pm 1.1 \times 10^{-4}$  M) indicated the expected shift of the H-3 methine proton, while a spectra of the sodium 3,5-dimethyl-4-nitrophenolate-cyclohexaamylose complex with the cavity 87% bound (assuming a dissociation constant of  $2.0 \times 10^{-1}$  M) did not indicate any shift in H-3 methine proton at all, implying it was not binding inside the cavity.

The sodium 2,6-dimethyl-4-nitrophenolate induced shifts in the cyclohexaamylose cavity are similar, although not identical to those we saw in the sodium *p*-nitrophenolate-cyclohexaamylose complex.

The shielding of the cycloamyloses H-3 methine protons is the same as that observed for the cycloamylose-sodium *p*-nitrophenolate complex; however, the H-5 methine protons are now strongly deshielded. The H-3 shielding is certainly due to the magnetic field of the aromatic  $\pi$  cloud. It may be that the 2,6-methyl groups of the substrate help to hold the nitro oxygens in the vicinity of the H-5 methine protons resulting in effective compression deshielding<sup>15</sup> or charge deshielding.<sup>16</sup>

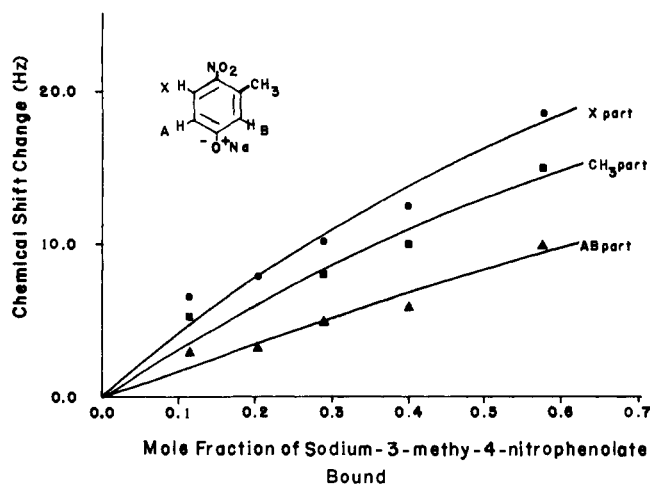


**Figure 4.** A plot of the change in chemical shifts of the aromatic and methyl protons of sodium 3-methyl-4-nitrophenolate vs. the percent-bound phenolate.

The effect of sodium 3,5-dimethyl-4-nitrophenolate on  $^1\text{H}$  NMR of cyclohexaamylose is far less pronounced and probably largely due to medium effects caused by the high concentration of substrate. Clearly the H-3 protons are not moving, although there may be some small amount of shielding of the H-5 protons.

**Cyclohexaamylose Binding of 3-Methyl-4-nitrophenol and Sodium 3-Methyl-4-nitrophenolate.** The changes in the visible spectra of both 3-methyl-4-nitrophenol and sodium 3-methyl-4-nitrophenolate were measured as a function of an increasing cycloamylose/substrate ratio. The sodium 3-methyl-4-nitrophenolate-cyclohexaamylose complex in pH  $11.00 \pm 0.02$  phosphate buffer ( $I = 0.5$ ) at  $25^\circ\text{C}$  has a  $K_D$  of  $4.2 \pm 0.4 \times 10^{-2}$  M. Hildebrand treatment of the data using a simple  $A + B \rightleftharpoons AB$  equilibrium model again resulted in an excellent data fit.

The visible spectra of various 3-methyl-4-nitrophenol-cyclohexaamylose mixtures in phosphate buffer at pH  $6.5 \pm 0.02$  ( $I = 0.5$ ) at  $25^\circ\text{C}$  indicated there was no complex formation corresponding to either an  $A + B \rightleftharpoons AB$  or  $AB + B \rightleftharpoons AB_2$  equilibrium model. Furthermore, visible spectral changes in the phenolic substrate were very small even at ratios of cyclohexaamylose/3-methyl-*p*-nitrophenol as high as 100. We were able to approximate changes in the visible spectra of the substrate simply by adding  $\alpha$ -D-glucose to the substrate at concentrations six times that of the cyclohexaamylose concentrations used.

The dissociation constant for the sodium 3-methyl-4-nitrophenolate-cyclohexaamylose complex was also measured with both NMR and optical polarimetry. The NMR experiment was run in  $\text{D}_2\text{O}$  with phosphate buffer at  $23 \pm 0.5^\circ\text{C}$  with pH  $11.00 \pm 0.02$ ,  $I = 0.5$ , yielding a  $K_D$  of  $3.5 \pm 0.16 \times 10^{-2}$  M. A plot of the change in chemical shifts of the aromatic and methyl protons vs. the percent-bound substrate shows that both the 3-methyl group and the meta protons sustain nearly twice the chemical change as the ortho hydrogens, implying substrate penetration is nitro end first (Figure 4).

The changes in the optical rotation of the cyclohexaamylose in phosphate buffer at pH  $11.0 \pm 0.02$ ,  $I = 0.5$ , as a function of an increasing sodium 3-methyl-4-nitrophenolate-cyclohexaamylose ratio suggested very weak binding. Even with a guest-to-host ratio of 50 ( $4 \times 10^{-4}$  M cyclohexaamylose and  $2 \times 10^{-2}$  M sodium 3-methyl-4-nitrophenolate), there was little change in optical rotation of the cyclohexaamylose. For a guest-to-host ratio of 10 ( $4 \times 10^{-4}$  M cyclohexaamylose and  $4 \times 10^{-3}$  M sodium *p*-nitrophenolate), under identical conditions there is a 69% increase in the optical rotation of the

substrate. The  $K_D$  for this complex is  $4.0 \pm 0.8 \times 10^{-4}$  M and therefore the substrate is 99% bound. If similar changes in rotation could be expected for sodium 3-methyl-4-nitrophenolate, then we would estimate the dissociation constant must be  $>10^{-1}$  for the changes we observed.

**Cyclohexaamylose Binding of 3,5-Dimethyl-4-nitrophenol and Sodium 3,5-Dimethyl-4-nitrophenolate.** The changes in the visible spectra of both 3,5-dimethyl-4-nitrophenol and sodium 3,5-dimethyl-4-nitrophenolate at pH  $6.5 \pm 0.02$  and pH  $11.0 \pm 0.02$ , respectively,  $I = 0.5$ , at  $25^\circ\text{C}$ , were measured as a function of added cycloamylose. Although the cycloamylose induced rather substantial hypochromic shifts in the substrate spectra, any attempt to fit these data to either an  $A + B \rightleftharpoons AB$  or an  $AB + B \rightleftharpoons AB_2$  equilibrium model using a Hildebrand treatment failed. In essence, simple binding did not occur. The binding of the sodium 3,5-dimethyl-4-nitrophenolate to cyclohexaamylose was also investigated polarimetrically. However, even at substrate-to-cycloamylose ratios of 87.5 ( $4.0 \times 10^{-4}$  M cyclohexaamylose,  $3.5 \times 10^{-2}$  M sodium 3,5-dimethyl-4-nitrophenolate in pH  $11.0 \pm 0.02$  phosphate buffer,  $I = 0.5$ , at  $25^\circ\text{C}$ ), no change in the optical rotation of the cyclohexaamylose was observed. To further substantiate that the sodium 3,5-dimethyl-4-nitrophenolate was not binding in the cavity, the dissociation constant for the cyclohexaamylose-sodium *p*-nitrophenolate complex ( $6.3 \times 10^{-4}$  M determined polarimetrically) was measured by optical rotation as previously described in the presence of three different concentrations of sodium 3,5-dimethyl-4-nitrophenolate, 0.007, 0.023, and 0.035 M, respectively. The apparent binding constants at each of these concentrations are  $1.0 \pm 0.18 \times 10^{-3}$ ,  $0.8 \pm 0.22 \times 10^{-3}$ , and  $1.2 \pm 0.21 \times 10^{-3}$  M, respectively. A plot of the "inhibitor" concentration vs. the apparent dissociation constant shows little, if any, binding of the 3,5-dimethyl-4-nitrophenolate (Figure 1). Furthermore, 220-MHz  $^1\text{H}$  NMR spectra of 0.002 M cyclohexaamylose and 0.045 M sodium 3,5-dimethyl-4-nitrophenolate in  $\text{D}_2\text{O}$ -phosphate buffer (pD 11.00,  $I = 0.5$ ) at  $25^\circ\text{C}$  verified that substrate penetration of the cycloamylose cavity did not occur. The cycloamylose H-3 methine protons are not shielded at all, and the H-5 methine proton shifts are very small (Figure 3).

$^1\text{H}$  NMR studies, however, did reveal that the substrate's ortho protons were shifting with increasing cycloamylose-to-substrate ratios. However, attempted fit of the shift data to the Hildebrand equation failed. Furthermore, a plot of the data in the form  $\Delta\delta$  vs. the cycloamylose-substrate molar ratios and/or comparison of the resulting curve with computer simulated plots for an  $A + B \rightleftharpoons AB$  system with different  $K_D$  values verifies that simple binding of the substrate in the cavity is not occurring (Figure 2).

## Discussion

**Measurements.** In this investigation, cycloamylose-substrate dissociation constants were determined with three independent techniques: nuclear magnetic resonance,<sup>7,17</sup> optical rotation,<sup>13</sup> and visible spectroscopy.<sup>18</sup> Furthermore, the binding constants were measured under two different sets of experimental conditions: holding the substrate concentration constant and varying the cycloamylose concentration as well as the inverse situation. Although it is clear that the application of any one of these methods would provide precise binding constants, together they give both a measure of the accuracy of the binding constants as well as a description of the cycloamylose-substrate disposition.

The  $^1\text{H}$  NMR changes experienced by both the host and guest molecules on complexation have made it possible to verify that the dissociation constants determined in these studies indeed represent binding of the substrate "in" the cyclohexaamylose cavity.

The optical rotation changes generated on cycloamylose-

substrate complexation result from both induced optical activity in the substrate<sup>19</sup> and changes in the conformation of the cavity.<sup>20</sup> We have shown that at the wavelength our measurements were made most of the optical rotation change can be ascribed to induced optical activity in the substrate.<sup>21</sup> However, the remainder of the change is probably due to cycloamylose conformational changes.

Our NMR studies suggest that such conformationally induced changes in optical rotation would result from widening of the cycloamylose cavity by movement of the glucose rings about the C-1-O-C-4' glycosidic bonds as the distortion in the component rings is minimal. The 100.1-, 220-, and 270-MHz NMR spectra reveal no obvious changes in any of the  $^1\text{H}$ -coupling constants for the complexes cyclohexaamylose implying that no significant distortion in the individual rings was occurring.

Although the cycloamylose coupling constants remain the same, we have shown that there are substantial changes generated in both the  $^{13}\text{C}$  and  $^1\text{H}$  NMR spectra of both the host and guest molecules on complex formation. In this investigation the changes in the  $^1\text{H}$  chemical shifts of the host and guest molecules are used to verify the strength of binding and the disposition between substrate and cavity.

From the observed changes in the chemical shifts for both the cyclohexaamylose host and the respective guest molecules, sodium *p*-nitrophenolate, sodium 2,6-dimethyl-4-nitrophenolate, sodium 3-methyl-4-nitrophenolate, and sodium 3,5-dimethyl-4-nitrophenolate, as well as from the known forward and reverse rate constants for similar cyclohexaamylose-substrate association equilibrium (e.g.,  $5.2 \times 10^8 \text{ M}^{-1} \text{ s}^{-1}$  and  $1.3 \times 10^5 \text{ s}^{-1}$ , respectively, for cyclohexaamylose-sodium *p*-nitrophenolate),<sup>1</sup> it is clear that the system is in the NMR chemical-shift fast exchange limit. This means that the various substrate proton resonances appear at the average of the chemical shift of free substrate and the substrate bound in each possible orientation to cyclohexaamylose, weighted by the fractional population of the substrate molecule in each environment. The same is, of course, true for the cyclohexaamylose molecule with each of its resonances occurring at its fast exchange position, weighted by the fraction of empty cyclohexaamylose molecules and the fraction of cyclohexaamylose's molecules which have guests.

In an earlier study on the cyclohexaamylose-sodium *p*-nitrophenolate complex employing both the changes in chemical shifts of the substrate and guest molecules on complexation and an intermolecular nuclear Overhauser effect, we were able to show that substrate penetration was asymmetric and only partial.<sup>6</sup> We were then able to associate the largest changes in chemical shifts of the substrate's protons with the portion of the aromatic ring penetrating the cycloamylose cavity, a finding which was extended to this investigation.

**Cycloamylose-Substrate Binding.** In principle, sodium *p*-nitrophenolate can penetrate the cyclohexaamylose cavity effectively in only two different orientations (Figure 5), either oxygen or nitro end first. A third orientation with penetrating ortho and meta positions is unreasonable, simply because very little of the substrate would fit into the cavity. However,  $^1\text{H}$  NMR studies clearly indicated that sodium *p*-nitrophenolate penetrated the cyclohexaamylose cavity at the wide 2,3-hydroxyl side nitro end first and only to the extent that the meta protons were in close proximity to the cycloamylose 3-H protons.

Just how important this orientation is to substrate binding is, of course, relevant to the nature of the binding forces. Two possibilities exist with respect to substrate orientation: either the sodium *p*-nitrophenolates or *p*-nitrophenols can only bind in the cavity nitro end first, or this orientation represents an energetically slightly more favorable disposition and, if steri-

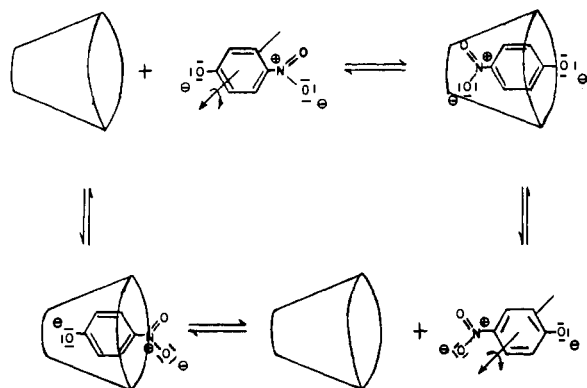


Figure 5. The two most likely dispositions for cycloamylose–sodium *p*-nitrophenolate complexes.

cally prohibited, the substrate can reorientate itself and penetrate the cavity hydroxyl end first and bind.

From the data in Table II, it is clear that the substrate can only bind in the cavity nitro end first. Using sodium *p*-nitrophenolate as the standard, introduction of methyl groups at the 2 and 6 positions of *p*-nitrophenol weakens binding only slightly by a factor of about 2.4. However, introduction of a single methyl group at the 3 position of *p*-nitrophenol weakens the binding substantially by a factor of about 100, while introduction of methyl groups at both the 3 and 5 positions completely inhibits binding by the usual mechanism. With the neutral compounds, introduction of methyl groups at the 2 and 6 positions of *p*-nitrophenol actually enhances binding slightly by about a factor of about 4; however, introduction of methyl groups at the 3 or at the 3 and 5 positions of *p*-nitrophenol prevents any binding of the substrate in the cavity. In each case, the phenol binds in the cavity more weakly than the corresponding anion. Sodium *p*-nitrophenolate binds about 130 times tighter than the phenol, sodium 2,6-dimethyl-4-nitrophenolate about 2 times more tightly than its phenol, while sodium 3-methyl-4-nitrophenolate has a  $K_D$  of  $1.23 \pm 0.39 \times 10^{-1}$  M and the corresponding phenol does not bind at all. Although solvation of the hydroxyl oxanion of the sodium *p*-nitrophenolates would be best served by having it point out into solution the neutral compounds should certainly be able to penetrate and bind in the cavity hydroxyl end first, but they do not. This means either the phenolic hydroxyl cannot penetrate the cavity for solvation reasons or the substrate dipole has strong orientational preference.

### Conclusion

The three different explanations for cycloamylose–substrate binding energy, release of cycloamylose strain energy,<sup>8</sup> release of high-energy cavity water, and London dispersion forces<sup>9,22</sup> interactions, can now be evaluated. Although the first two proposals are somewhat difficult to separate because they predict similar phenomenological results, the third concept is easy to partition from the first two. Both the strain energy and high-energy water theories suggest that no matter how the substrate penetrates the cavity, as long as it relieves the ring strain or displaces the high-energy cavity water, it should bind. They also suggest that the more effective a substrate is at performing these tasks, the tighter it should bind. For example, the observation that benzoic acid binds about 90 times more effectively in the cavity than phenol would be explained by assuming benzoic acid penetrates the carboxyl group first, just as the phenol would be expected to penetrate the hydroxyl end first, but the carboxyl group is more effective at “filling the cavity”.

However, the binding constants for the *p*-nitrophenol–cyclohexaamylose and the *p*-nitrobenzoic<sup>23</sup> acid–cyclo-

Table II. Cyclohexaamylose–Substrate Dissociation Constants

Substrate	$K_D$ (UV 25 ± 0.1 °C), M	$K_D$ (NMR 23 ± 0.5 °C), M	$K_D$ (opt. rot. 25 ± 0.1 °C), M
	$5.3 \times 10^{-2}$		
	$4.0 \pm 0.8 \times 10^{-4}$	$3.7 \pm 0.2 \times 10^{-4}$	$6.3 \pm 0.4 \times 10^{-4}$
	$1.76 \pm 0.18 \times 10^{-3}$		
	$9.42 \pm 1.1 \times 10^{-4}$	$1.96 \pm 0.53 \times 10^{-4}$	$1.42 \pm 0.58 \times 10^{-3}$
	N.B.		
	$4.2 \pm 0.4 \times 10^{-2}$	$3.5 \pm 0.16 \times 10^{-2}$	$>10^{-1}$
	N.B.		
	N.B.	N.B.	N.B.

hexaamylose complexes reveal some disturbing inconsistencies. The *p*-nitrophenol binds in the cavity more tightly than the phenol while the *p*-nitrobenzoic acid binds more weakly than benzoic acid. Although the nitro group of the *p*-nitrophenol would “fill the cavity” somewhat more effectively and therefore the phenol would bind more tightly, the fact that *p*-nitrobenzoic binds more weakly than benzoic acid defies any explanation of this type. Furthermore, neither theory suggests that *p*-nitrophenolate anions should bind more tightly than the corresponding neutral species.

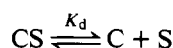
Our findings are also very difficult to rationalize in terms of both the high-energy water picture as well as in terms of the strain energy model. It is clear that *p*-nitrophenol-like substrates are willing to bind in the cavity in only one orientation, nitro end first, and anything that prevents this weakens binding substantially. Furthermore, we continue to see the *p*-nitrophenolate anions binding more tightly than the corresponding neutral compounds. After consideration of all these findings, the picture that emerges is one which minimizes the importance of both high-energy cavity solvent and strain energy and amplifies the role of London dispersion forces. It is, of course, important to recognize that the London dispersion forces' contribution to the overall binding energy will vary with the

dipolar nature of the substrate and, thus, will be less important for less polar substances.

**Acknowledgment.** Acknowledgment is made to the donors of the Petroleum Research Fund, administered by the American Chemical Society, for support of this research. We also wish to acknowledge Dr. Peter McPhie and Dr. Sherry Fisk of the National Institutes of Health for their assistance with the computerized curve fitting and 220-MHz NMR spectra and M. Meeley for her technical assistance.

## Appendix A

From the observed changes in the chemical shifts for both the *p*-nitrophenolate guest and the cyclohexaamylose host as the host:guest ratio was varied, as well as from the known formation and dissociation rate constants for the parent sodium *p*-nitrophenolate compound ( $5.2 \times 10^8 \text{ M}^{-1} \text{ s}^{-1}$  and  $1.2 \times 10^5 \text{ s}^{-1}$ , respectively),<sup>24</sup> the system is in the NMR chemical-shift fast-exchange limit.<sup>25</sup> This means the substrate resonances appear as the average of the chemical shift of free *p*-nitrophenolate and the chemical shift of *p*-nitrophenolate bound in each possible orientation to cyclohexaamylose, weighted by the fractional population of substrate molecules in each environment. The same applies to the cyclohexaamylose resonances where the resonance positions are weighted by the fraction of "empty" molecules and by the fraction of cyclohexaamylose molecules which have guests. With these facts on hand, it is possible then to measure the dissociation constant for the cyclohexaamylose complexes by observing the changes in chemical shift of the substrate (S) protons as a function of added cycloamylose (C). Consider the equilibrium expression:



$$K_d = [S][C]/[CS] \quad (1)$$

$$C_0 = C + CS \quad (2)$$

$$S_0 = S + CS \quad (3)$$

$$K_d = \frac{[S_0 - CS][C_0 - CS]}{[CS]} \quad (4)$$

The observed chemical shift will be given by:

$$\delta_{\text{obsd}} = \frac{S}{S_0} \delta_S + \frac{CS}{S_0} \delta_{CS} \quad (5)$$

Combining eq 2 and 4 produces:

$$\delta_{\text{obsd}} = \frac{(S_0 - CS)\delta_S}{S_0} + \frac{CS}{S_0} \delta_{CS} \quad (6)$$

The change in chemical shift is given by:

$$\Delta\delta = \delta_{\text{obsd}} - \delta_S \quad (7)$$

Combining eq 5 and 6 gives:

$$\Delta\delta = \left( \delta_S - \frac{CS}{S_0} \delta_S - \frac{CS}{S_0} \delta_{CS} \right) - \delta_S$$

which on rearrangement transforms to:

$$\Delta\delta = \frac{CS}{S_0} (\delta_{CS} - \delta_S)$$

Letting  $\delta_{CS} - \delta_S = Q$ , CS is expressed as:

$$\Delta\delta S_0 / Q = CS \quad (8)$$

Equation 3 is now rearranged to:

$$K_d[CS] = (CS)^2 - C_0CS - S_0CS + C_0S_0 \quad (9)$$

and it is possible to solve for  $K_d$  two different ways. Equation 8 can be combined with eq 7 directly and the  $K_d$  solved by computer analysis or eq 8 can be put in a form to allow for simple graphing. Experimentally this is limiting because  $[CS]^2 \ll C_0S_0$  which transforms eq 8 to:

$$\therefore K_d[CS] = C_0S_0 - C_0CS - S_0CS \quad (10)$$

Substituting eq 7 into eq 9 and rearranging generates:

$$\frac{K_d}{Q} + \frac{C_0 + S_0}{Q} = \frac{C_0}{\Delta\delta}$$

Our experimental conditions did not conform in every case to the  $[CS]^2 \ll C_0S_0$  requirement for a linear plot. Equations 7 and 8 were combined and expressed in the form below:

$$f_i(QK_d) = C_0^i S_0^i - \frac{(C_0^i S_0^i \Delta\delta^i - S_0^{i2} \Delta\delta - K_d S_0^i \Delta\delta^i)}{Q} + \left( \frac{S_0^i \Delta\delta^i}{Q} \right)^2$$

where  $i = 1, 2, 3 \dots n$ .

The  $Q$  values were estimated from plots of the change in chemical shift vs. increasing cycloamylose-substrate ratios and the ranges for the  $K_D$  values were taken from the other techniques. A computer analysis was effected on this expression for  $S_0^i$ ,  $C_0^i$ , and  $\Delta S_0^i$  to minimize the absolute value of  $\sum |f - f_i|$  where  $f(QK_D)$  is zero.

## References and Notes

- (1) F. Cramer and H. Hettler, *Naturwissenschaften*, **54**, 625 (1967).
- (2) D. W. Griffiths and M. L. Bender, *J. Am. Chem. Soc.*, **95**, 1679 (1973).
- (3) B. Siegel and R. Breslow, *J. Am. Chem. Soc.*, **97**, 6869 (1975).
- (4) Y. Iwakura, K. Uno, F. Toda, S. Onozuka, K. Hattori, and M. L. Bender, *J. Am. Chem. Soc.*, **97**, 4432 (1975).
- (5) Y. Kitawa and M. Bender, *Bioorg. Chem.*, **4**, 237 (1975).
- (6) R. Bergeron and R. Rowan, *Bioorg. Chem.*, **5**, 290 (1976).
- (7) R. Bergeron and M. Channing, *Bioorg. Chem.*, **5**, 289 (1976).
- (8) P. C. Manor and W. Saenger, *J. Am. Chem. Soc.*, **96**, 3690 (1974).
- (9) D. W. Griffiths and M. L. Bender, *Adv. Catal.*, **23**, 209 (1973).
- (10) R. Adams and H. W. Stewart, *J. Am. Chem. Soc.*, **63**, 2859 (1941).
- (11) R. G. Bates, "Determination of pH; Theory and Practice", Wiley, New York, N.Y., 1956.
- (12) H. A. Benesi and J. H. Hildebrand, *J. Am. Chem. Soc.*, **71**, 2703 (1949).
- (13) C. Formoso, *Biopolymers*, **13**, 909 (1974).
- (14) P. V. Demarco and A. L. Thakker, *Chem. Commun.*, **2** (1970).
- (15) B. V. Cheney, *J. Am. Chem. Soc.*, **90**, 5386 (1968).
- (16) H. Booth and A. H. Bostoch, *Chem. Commun.*, 637 (1967).
- (17) J. P. Behr and J. M. Lehn, *J. Am. Chem. Soc.*, **98**, 1743 (1976).
- (18) R. L. Van Etten, J. F. Sabastlan, G. A. Clowes, and M. L. Bender, *J. Am. Chem. Soc.*, **89**, 3242 (1967).
- (19) K. Harata and H. Uedaria, *Nippon Kagaku Zasshi*, **48**, 375 (1975).
- (20) D. A. Rees, *J. Chem. Soc. B*, 877 (1970).
- (21) R. J. Bergeron and P. McPhie, submitted for publication to *Tetrahedron*.
- (22) E. A. Lewis and L. D. Hansen, *J. Chem. Soc., Perkin Trans. 2*, 2081 (1973).
- (23) B. Casu and L. Rava, *Ric. Sci.*, **36**, 733 (1966).
- (24) F. Cramer, W. Saenger, and H. Spatz, *J. Am. Chem. Soc.*, **89**, 14 (1967).
- (25) B. D. Sykes and M. D. Scott, *Ann. Rev. Biophys. Bioorg.*, **1**, 27 (1972).